RSC Advances

ROYAL SOCIETY OF CHEMISTRY

www.rsc.org/advances

Journal Name

RSCPublishing

ARTICLE

One-pot synthesis of Au/Ag bi-metallic nanoparticles to modulate the emission of CdSe/CdS quantum dots

Cite this: DOI: 10.1039/x0xx00000x

Kun Jia,*[a,c] Liting Yuan,[a,c] Xuefei Zhou,[a] Lin Pan,[a] Pan Wang,[a] Wenjin Chen,[b] and Xiaobo Liu*[a]

Received 00th January 2012,
Accepted 00th January 2012

DOI: 10.1039/x0xx00000x

www.rsc.org/

In this work, the gold/silver bimetallic nanoparticles (Au/Ag NPs) have been synthesized via a facile one-pot protocol involving co-reduction of chloroauric acid and silver nitrate with *N, N*-dimethylformamide (DMF) solvent in the presence of water soluble polyvinylpyrrolidone (PVP). The morphology of obtained Au/Ag NPs can be readily modified by changing reaction time and relative concentration ratio of gold/silver precursor. Subsequently, the synthesized Au/Ag NPs have been employed to modulate the fluorescent emission of CdSe/CdS quantum dots (QD) in the solution phase on the basis of plasmon controlled fluorescence. The experimental results demonstrated that the fluorescent emission of CdSe/CdS QD can be either obviously quenched or enhanced, depending on the spectral overlap and local distances control between CdSe/CdS QD and Au/Ag bimetallic NPs. Specifically, the as-synthesized Au/Ag NPs significantly quenched the fluorescent emission of CdSe/CdS QD and the quenching effect was enhanced when the plasmonic wavelength of Au/Ag NPs was tuned towards fluorescent emission wavelength of CdSe/CdS QDs. On the contrary, the fluorescent emission of CdSe/CdS QD can be obviously enhanced in the presence of SiO_2 coated Au/Ag NPs with appropriate layer thickness.

Introduction

Owing to their fascinating near field and far field optical properties, noble metal (especially for gold and silver) nanostructures have attracted tremendous research interests both in academic and industrial fields.[1-5] Localized surface plasmon resonance (LSPR), derived from the collective oscillation of free electrons of noble metal nanostructures excited by incident light, is the fundamental principle responsible for their rich optical properties. The LSPR wavelength, depending on the nanostructures morphology (size, shape, aspect ratio, etc.), composition and local dielectric micro-environments, plays an important role in many plasmon modulated optical transitions.[6-9] Generally, the typical plasmonic wavelength of silver nanospheres is located in the range of 400-450 nm, while the gold nanostructures show representative extinction peak in the longer wavelength range of 500-600 nm. Moreover, the anisotropic nanostructures (nanocubes, nanorods, nanoplates, nanowires, etc.) normally display more complex plasmonic spectra due to the activation of high order plasmonic modes when compared with isotropic nanospheres. Therefore, increasing research efforts have been devoted into the synthesis and application of anisotropic nanostructures in the nanoscale location, orientation and manipulation of electromagnetic waves beyond the diffraction limit.[10, 11]

Among various plasmonic mediated optical transitions, plasmon modulated fluorescence has witnessed thriving development recently, mainly due to the widespread application of fluorescent spectroscopy in biomedicine, diagnostics, bio/chem-detection and photo-electronic devices, etc.[12] In addition, the fluorescent emission can be detected from a large amount of different materials (such as organic dyes, conjugated polymers, quantum dots, metal nanoclusters, rare earth compounds, etc.) and the emitted fluorescence can be effectively quenched, enhanced or spectral modulated when these fluorophores are located around the plasmonic nanostructures.[13-15] Especially, the quantum dots (QD) consisting of small sized semiconductor nanocrystals exhibit highly tunable fluorescent emission due to the confined excitons in all three dimensions, moreover they have large Stokes shift, high quantum yields, narrow emission spectra and

ability to generate multi-color fluorescence under a single excitation wavelength, which leads to their potential applications in biomedicine, solar energy harvesting and optoelectronic devices.[16-20] Therefore, the combination of plasmonic nanostructures and quantum dots would further expand the photoluminescent properties of these nanohybrids by virtue of photon-exciton interaction.

It has been reported that the photon-exciton interaction between plasmonic nanostructures and semiconductor nano-emitters are dependent on several key factors, such as local distance between QD and metal nanoparticles (MNP) surface, excitation polarization, spectra overlap between QD excitation/emission wavelength and LSPR band of plasmonic metal nanostructures.[21-25] The fluorescent emission wavelength and LSPR band can be finely tuned by the geometry (size and shape) of QD and metal nanoparticles respectively, while the local distance between QD and metal nanostructures is controlled by different surface chemical modification protocols, electron-beam lithography and unconventional lithography.[26] While the latter two methods require either expensive instruments or are time consuming, the surface chemical modification strategies not only allow the interparticle distance control, but also are able to control the QD-MNP interaction in a much easier and flexible manner. For instance, the various QD-MNP nanohybrids with enhanced photoluminescence have been fabricated by introducing silica shells, complementary oligonucleotides or oppositely charged polyelectrolytes spacer layers to avoid the strong quenching effects.[27-31] However, most of these QD-NMP nanohybrids with plasmon enhanced fluorescence have been fabricated on the solid substrate and using isotropic nanospheres, only few works have reported the enhanced fluorescence of QD by using surface modified MNPs in aqueous solution so far,[32-35] while the anisotropic gold or silver nanoparticles enhanced fluorescence of QD in the solution phase was not yet reported according to our best knowledge. Moreover, it has been demonstrated in several recently published work that the plasmonic, luminescent and catalytic properties of gold can be effectively enhanced thanks to the "silver effects", which implies that the bimetallic gold/silver alloy or core-shell nanoparticles exhibit improved performance in various plasmon-mediated optical transitions compared to the gold or silver monometallic nanostructures.[36-38]

In this work, the gold/silver nanocubes (Au/Ag NPs) were synthesized in the common organic solvent of *N, N*-dimethylformamide (DMF) in the presence of water soluble polymer polyvinylpyrrolidone (PVP). The experimental results demonstrated that the initial concentration ratio of gold/silver precursors played an important role in shaping the morphology of obtained gold/silver nanocubes. Subsequently, the highly luminescent CdSe/CdS core-shell QD have been synthesized and their photoluminescent wavelength was tuned in the vicinity of plasmonic extinction wavelength of as-synthesized Au/Ag NPs and silica modified Ag/Au NPs, in order to determine the plasmon mediated fluorescence of QD in terms of spectra overlap and interparticle distance in the solution phase.

Experimental section

Synthesis of gold/silver nanoparticles (Au/Ag NPs).

The Au/Ag NPs were prepared at different molar ratios of $HAuCl_4$ and $AgNO_3$, using DMF and PVP as the reduction and stabilization agent, respectively. In a typical synthesis, 2 g PVP (K30, Sigma) were dissolved in 50 mL DMF solvent and stirred continuously under nitrogen protection, then mixed aliquots of $AgNO_3$ and $HAuCl_4$ aqueous solutions (0.2 M, total volume of 250 μL) with different relative concentration ratios were subsequently added into the PVP/DMF solution, followed by refluxing the reaction mixture at 156 °C for 1 h, finally the synthesized Au/Ag nanoparticles were separated and purified by repeated centrifugation and washing for three times.

Silica modification of Au/Ag NPs.

The as-synthesized Au/Ag NPs were dispersed in 15 mL ddH_2O supplemented with 1.5 mL ammonia, followed by addition of 50 mL isopropanol under vigorous stirring. Afterwards, 80 μL tetraethoxysilane was dissolved in 3 mL isopropanol and separately added into the previous reaction mixture in 6 times, then the reaction solution were stirred at room temperature for 6 h, 12 h, and 24 h, respectively, followed by centrifugation and washing, to finally obtain the Au/Ag@SiO_2 NPs with different silica layer thicknesses.

Synthesis of CdSe/CdS core-shell QD.

The CdSe/CdS QD were prepared by a one-pot continuous thermal decomposition method. Specifically, cadmium precursor solution was prepared by dissolving 0.26 g cadmium oxide (CdO) in 2 mL mixture of oleic acid and liquid paraffin at 180 °C, then 1 mL cadmium precursor solution was added into 9 mL liquid paraffin solubilized with 4 mg selenium powder and stirred at 220 °C for 5 min to obtain CdSe QD. Next, 12 mg sodium sulfide ($Na_2S•9H_2O$) was introduced into the as-synthesized CdSe QD solution, where the excess cadmium precursor was compounded with sodium sulfide at 80 °C for 30 min to form the CdS shell on the CdSe core nanocrystals. Finally, the as-prepared CdSe/CdS core-shell QD was dispersed in chloroform/methanol mixed solvent (volume ratio of 1:3) and purified by repeated centrifugation and washing.

Preparation of water soluble CdSe/CdS QD.

The water soluble QD was prepared after a simple phase transfer process. The previously purified CdSe/CdS QD was firstly dispersed in 4 mL chloroform, followed by addition of 0.5 mg sodium thioglycolate and vigorous stirring for 12 h at room temperature, then 500 μL NaOH aqueous solution (20%) and 5 mL ddH_2O were introduced and the mixture solution was allowed to separate into two layers without any stirring. Lastly, the resulted upper layer solution was centrifuged and washed with acetone several times to thus obtain the water soluble CdSe/CdS QD.

Samples characterization and measurement.

The UV-Vis spectra of as-synthesized Au/Ag NPs, Au/Ag@SiO_2 NPs and CdSe/CdS QD were recorded using a Persee TU 1901 UV-Vis spectrophotometer. X-ray photoelectron spectroscopy (XPS) spectra for synthesized Au/Ag nanoparticles were recorded on a PHI-5300 ESCA spectrometer (Perkin–Elmer). The surface morphology of Au/Ag NPs and QD were characterized with field-emission scanning electron microscope (SEM, JEOL, JSM-6490LV) and transmission electron microscope (TEM, JEOL, JEM-2100F), respectively. The steady state and transient state fluorescent spectroscopy (fluorescent decay and lifetime determination) of

Au/Ag NPs and QDs hybrids were tested using a fluorescent spectrophotometer (F-4600, Hitachi) and Horiba Jobin Yvon Tempro-01 instrument, respectively. The photos of various solution samples in vials under white light and UV light illumination were captured using a DSLR camera (Nikon D7000). For the fluorescent quenching and enhancement experiments, all the samples were mixed uniformly in a quartz cuvette and incubated for 5 min prior to fluorescent measurement.

Results and discussion

Owing to their unique ability to modulate light-mater interactions, heterogeneous bimetallic gold/silver nanoparticles exhibit enhanced optical, electronic, catalytic properties when compared with their monometallic counterparts.[39] Normally, the shape-controlled Au/Ag heterogeneous nanostructures have been synthesized via the galvanic replacement reactions,[40] seed-mediated growth,[41] thermal annealing process[42] and simultaneous reduction of two metal ions.[38, 39] In the former two protocols, the well-faceted seeds nanoparticles formation and subsequent secondary metal deposition on seeds surface were separated into two or more independent processes, thus it requires tedious experimental work to modulate the morphology evolution of Au/Ag bimetallic NPs. While the thermal annealing was assumed as an effective way to prepare heterogeneous bimetallic Au/Ag NPs, the obtained bimetallic nanoparticles were basically isotropic (i.e. nanospheres).[42] On the contrary, the co-reduction of metal ions precursor in one-pot reaction was considered as a promising protocol to prepare anisotropic bimetallic gold/silver nanoparticles in a much easier way. In our previous work,[43] the highly luminescent silver nanoparticles with average size of 6 nm were synthesized in the common polar solvent of DMF in the presence of water soluble polymer of PVP, which demonstrated that the silver ions can be readily reduced by DMF to nanoparticles that were stabilized with PVP. Herein, we found that the morphology of prepared nanostructures can be dramatically shaped when small amount of $HAuCl_4$ precursor solution was introduced into the $AgNO_3$/PVP/DMF reaction system under the same experimental conditions.

Firstly, the reaction time influence on the extinction spectra of bimetallic Au/Ag nanostructures was determined, as shown in Fig.1a, a well-defined LSPR peak was detected for all the samples prepared with different reaction time, and the LSPR wavelength of Au/Ag bimetallic NPs (initial molar concentration of $[AgNO_3]$: $[HAuCl_4]$ = 9:1) was firstly redshifted from 412 nm to 430 nm after 40 min reaction, then blue-shift back to 410 nm after 60 min reaction. The TEM images of synthesized Au/Ag nanoparticles corresponding to three different reaction time of 10 min, 40 min and 50 min were displayed in Fig. 1b-d, clearly indicating that the initial increasing and followed decreasing of nanoparticles size. Moreover, this evolution of LSPR band with the reaction time for Ag/Au bimetallic NPs would be attributed to the chemical etching of pre-formed large sized Au/Ag bimetallic NPs, which was also observed in our previous work of monometallic luminescent silver nanoparticles.[43]

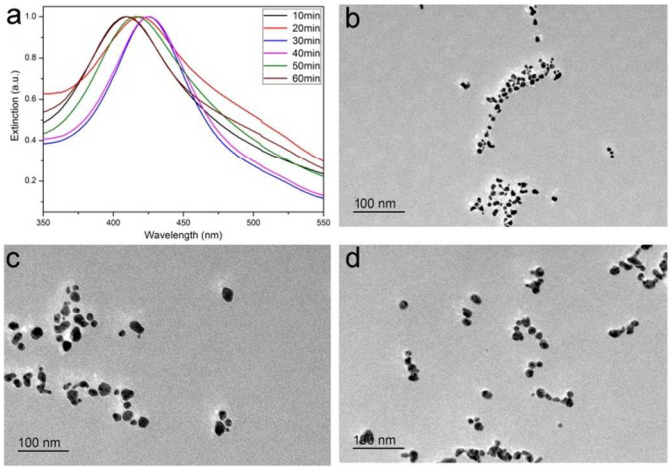

Fig. 1 The UV-Vis spectra (a) of Au/Ag bi-metallic nanoparticles synthesized in DMF solution under N_2 atmosphere for different time, the initial mole concentration ratio of $[AgNO_3]$: $[HAuCl_4]$ was 9:1, the mole concentration of PVP was 0.1 M and the transmission electron microscope morphology of Au/Ag nanoparticles after 10 min (b), 40min (c) and 50 min (d), respectively.

Next, the influence of two precursor concentration ratio onto the optical spectra and morphology of Au/Ag bimetallic nanostructures was investigated. As shown in Fig. 2a, when three different molar concentration ratios of $[AgNO_3]$: $[HAuCl_4]$ (9:1, 8:2, 6:4) were used in the synthesis, the LSPR band of obtained Au/Ag bimetallic nanostructures was red-shifted as the increasing dose of gold precursor solution. For instance, the LSPR resonant wavelength for $[AgNO_3]$: $[HAuCl_4]$ =9:1 was recorded at 420 nm, which was increased to 450 nm and 550 nm for the samples synthesized with 20 % and 40 % $HAuCl_4$ dosages, respectively, thus the three typical samples were accordingly named as Ag@Au420, Ag@Au450 and Ag@Au550. The FE-SEM was employed to characterize the morphology of obtained Au/Ag bimetallic nanoparticles; it was found that the monodispersed Ag/Au bimetallic nanocubes (Au/Ag NC) with average edge size of 150 nm were formed for Ag@Au420 sample (Fig. 2b), while the irregular and much larger Au/Ag bimetallic nanoparticles were imaged from the other two samples of Ag@Au450 and Ag@Au550 (Fig. 2 c, d).

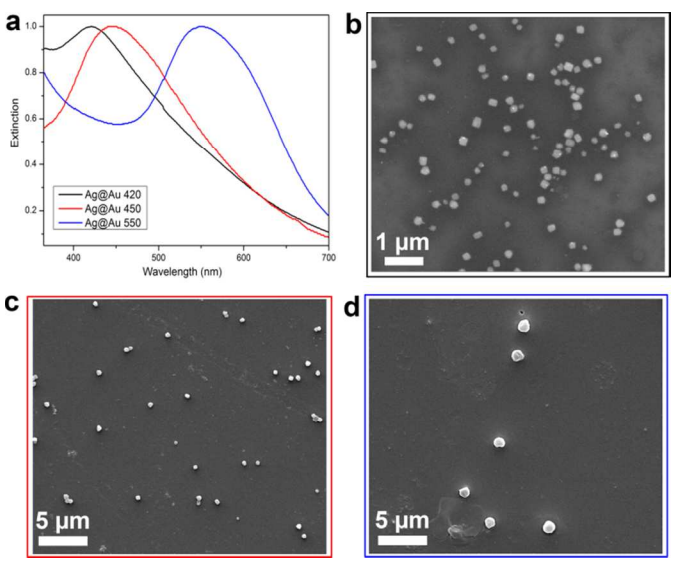

Fig. 2 The UV-Vis spectra (a) and SEM images (b-d) of three typical Au/Ag bi-metallic NPs, the relative mole concentration ratio of [AgNO3]: [HAuCl4] was 9:1, 8:2, 6:4 in the synthesis of Ag@Au 420, Ag@Au 450, Ag@Au 550 NPs, respectively.

In addition, the X-ray photoelectron spectroscopy was used to probe the chemical composition of bimetallic Au/Ag NPs. It was clear from Fig. 3 that the typical signals of silver $3d_{5/2}$ (368.4 eV), $3d_{3/2}$ (374.4 eV) and gold $4f_{1/2}$ (84.0 eV), $4f_{5/2}$ (87.7 eV) were both detected for Ag@Au420 sample, and the atomic concentration ratio of gold to silver calculated from XPS spectra was 17.1 %, which was quite close to the initial value of $HAuCl_4$ to $AgNO_3$ (16.9 %). However, for the other two large sized samples of Ag@Au450 and Ag@Au550, the intensity of gold signals in XPS pattern was much smaller than that of silver. Considering the XPS is a surface sensitive technique, these experimental results indicated that only small quantity of gold was presented on the surface of bimetallic Ag@Au nanoparticles. On the other hand, we found that the Au/Ag bimetallic nanoparticles yield was also decreased as the $HAuCl_4$ loading content increased, which implied that the co-reduction process by DMF was strongly inhibited by the high concentration of $HAuCl_4$. The previously published work by Pastoriza-Santos also reported that the chemical reduction of $HAuCl_4$ by DMF was quite difficult.[44] However, the presence of small quantity of $HAuCl_4$ was indispensable for the controlled synthesis of bimetallic anisotropic nanocubes, as only isotropic silver nanospheres were obtained in the absence of gold precursors according to our previous work.[43] Since the silver ions are easier to be reduced compared to gold ions, we assume that the silver nanospheres are obtained at the beginning of the reaction, which was then chemically etched by NO^{3-} and Cl^- from $AgNO_3$ and $HAuCl_4$ to form bimetallic nanoparticles. The chemical etching effects of NO^{3-} and Cl^- to silver nanoparticles have been well documented by several works as well.[40, 45, 46] Based on these optical and morphological characterization, we found that the nearly monodispersed Au/Ag bimetallic NPs can be readily prepared by reducing $AgNO_3$ in the presence of small quantity of $HAuCl_4$ in DMF/PVP mixture via one-pot reaction.

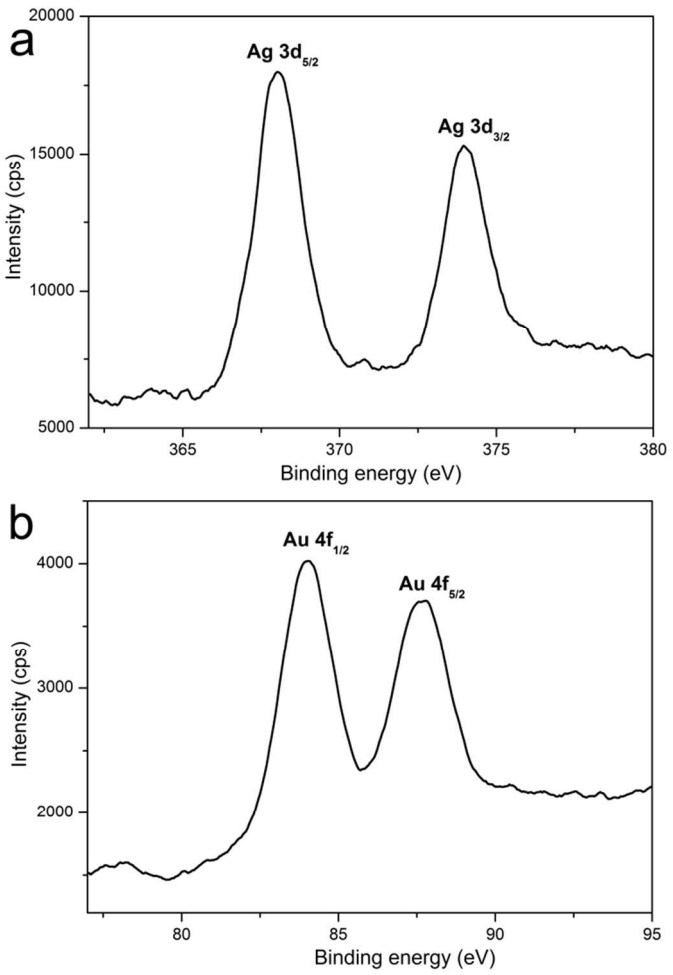

Fig. 3 The XPS spectra of silver 3d (a) and gold 4f (b) for the Ag@Au 420 bimetallic NPs.

It is well-known that the bimetallic Au/Ag nanostructures show enhanced optical near-field properties of absorption and scattering, moreover the bimetallic systems exhibit strong radiative properties due to the fact that silver is less lossy compared to gold. These fascinated optical properties allow bimetallic Au/Ag nanoparticles to play an active role in the modulation of fluorescent emission of various fluorophores via the fluorescent resonant energy transfer (FRET) or nanometal surface energy transfer (NSET) process.[47, 48] Additionally, the spectral overlap between LSPR band of plasmonic nanostructures and excitation/emission wavelength of fluorophores was reported to be an essential parameter in these plasmon mediated fluorescence, especially for the experiments conducted in the solution phase.[49] Fortunately, semiconductor nanocrystals QD can be excited in a wide range wavelength to emit fluorescence with a quite narrow wavelength, and their fluorescent emission wavelength can be readily tuned by controlling the size and morphology of QD, thus the QD can be employed as ideal fluorophores in the plasmon modulated fluorescent experiments. Therefore, we have synthesized the

highly luminescent green-emitting CdSe/CdS QD with a narrow fluorescent emission spectra (peaked at 530 nm, FWHM=31 nm) when excited with 365 nm UV light (see Fig. 4a), the ultra-small sized (~2 nm) spherical morphology were captured for the synthesized QD using a high resolution transmission electron microscope (HRTEM) as shown in Fig. 4b. In addition, the synthesized QD presented polycrystalline structures according to the selected area electron diffraction (SAED) patterns shown in inset of Fig. 4b.

On the other hand, although several plasmonic nano-emitters with enhanced luminescent properties were obtained by controlling the distance between semiconductor QD and metallic nanostructures with different spacer layers such as silica modification, polyelectrolytes or DNA oligonucleotides,[13, 23, 50, 51] the photoluminescent properties of these QD/Au/Ag hybrid nanostructures were characterized on solid substrates, less attention has been paid to their photoluminescence in colloid solution. Actually, the majority of (bio)chemical sensing experiments based on QD/Au/Ag hybrid nanostructures were conducted in liquid medium, thus herein the fluorescent emission profile of synthesized CdSe/CdS QD in the presence of previously prepared three Ag/Au bimetallic nanostructures was recorded in the solution phase to determine the plasmonic effects on the QD fluorescence.

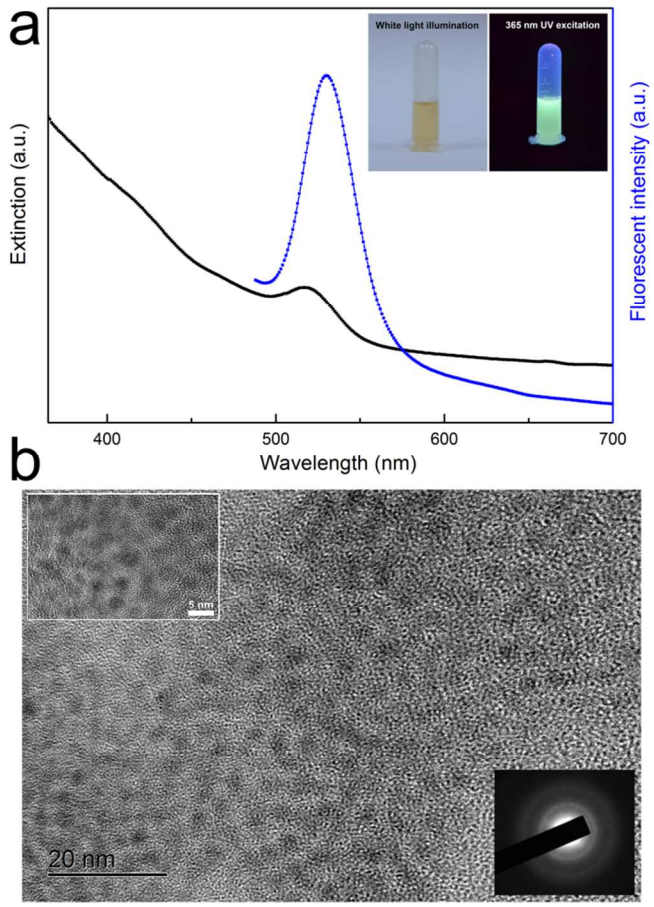

Fig. 4 The extinction, fluorescent emission spectra (a) and high resolution transmission electron microscope images (b) of synthesized QDs, the select area electron diffraction pattern of QDs was shown in inset.

Firstly, it was found that the fluorescent emission of CdSe/CdS QD was obviously quenched when the as-synthesized Ag/Au nanoparticles were added as shown in Fig. 5. More interestingly, the fluorescent quenching efficiency was enhanced with the increased size of Ag/Au NPs. For instance, the fluorescent emission intensity (integrated area under fluorescent peak from 500 nm to 600 nm, the same for the following section) of CdSe/CdS QD was quenched by 40 %, 51 % and 68 % when 40 % (volume ratio) Ag/Au@420, Ag/Au@450 and Ag/Au@550 was added, respectively. The detailed fluorescent intensity of QD and QD/Ag-Au NPs mixtures of different concentration ratios were summarized in Table 1. In addition, the fluorescent quench efficiency of QD by Ag/Au NPs was calculated as A/A_0, where A and A_0 represented the integrated fluorescent intensity of QD in the presence and absence of Au/Ag NPs, respectively, and the Stern-Volmer plots showing the variation of fluorescent quenching efficiency versus Au/Ag NPs concentration was presented in Fig. 5d, a good linearity was obtained for all the three samples and the maximum fluorescent quenching efficiency was obtained for the sample Ag@Au550 that had largest spectral overlap with fluorescent emission spectra of QD. These experimental results demonstrated that the QD fluorescent quenching by Au/Ag NPs was mainly due to the energy transfer from QD donors to Ag/Au NPs acceptor, which was also confirmed by the obvious decreasing of QD lifetime in the presence of Au/Ag NPs (see Table 1). Therefore, the more overlapped between LSPR band and fluorescent emission spectra, the higher energy transfer efficiency will be established, thereby leading to a stronger fluorescent quenching of QD by Au/Ag NPs.

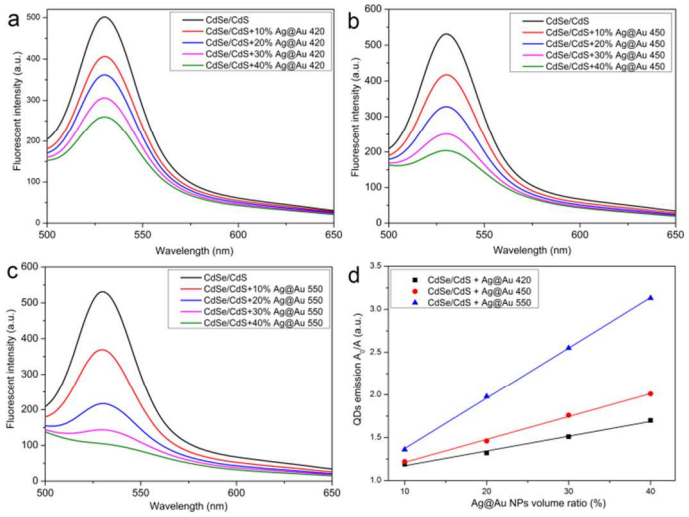

Fig. 5 The fluorescent emission of QDs in the presence of different sized Au/Ag NPs (a-c) and fluorescent quenching curves of CdSe/CdS QDs and Au/Ag NPs.

Table 1 The fluorescent intensities and lifetime of various CdSe/CdS QD and Au/Ag bimetallic NPs mixtures with different relative concentration ratios.

	QD	QD + 40%Ag@Au 450	QD + 40%Ag@Au 500	QD + 40%Ag@Au 550
Fluorescent intensity	28771	16967	14292	9197
Lifetime decrease (ns)	-	5.59 →3.89	5.77 → 3.84	5.80 → 4.18

On the contrary to the strong fluorescent quenching effects of QD by the pristine Au/Ag NPs, the appropriated surface modified Au/Ag NPs (such as silica modified metal nanostructures) can be employed to enhance the fluorescence of CdSe/CdS QD, leading to the so-called metal enhanced fluorescence (MEF) that has been well-documented in many published works.[21, 25, 26, 50, 52] The majority of MEF experiments were designed to precisely control the local distance between plasmonic nanostructures and fluorophores on a substrate, while only few works reported the MEF in solution phase so far. Generally, the fundamental principle for the MEF has been attributed to the strong local electric field enhancement effects derived from the plasmonic resonance of metal nanostructures, thus the LSPR extinction wavelength was considered as an essential factor in MEF experiments. In our experiments, the CdSe/CdS fluorescence was excited using 365 nm UV light, thus the monodispersed Ag@Au420 nanoparticles sample, with strongest enhanced electrical field in the excitation wavelength range of QD, was employed to conduct the MEF experiments in the aqueous solution. Firstly, the previously prepared CdSe/CdS QD in nonpolar solvent (hexane) was transferred into aqueous phase by using a phase-transfer agent of sodium thioglycolate (see details in experimental section), resulting to a red-shift of fluorescent emission wavelength to 560 nm. The red-shift of fluorescent emission CdSe/CdS QD before and after phase-transfer reaction was also confirmed by the solution color changing from green to yellow, and the fluorescent emission of the water-soluble CdSe/CdS QDs were again quenched by the unmodified Au/Ag NPs as shown in Fig. 6a. Then, the Au/Ag NPs were surface modified with different thicknesses of SiO_2 layer, which was confirmed by the steady red-shift of plasmonic extinction wavelength (Fig. 6b). When these SiO_2 modified Au/Ag NPs aliquots were mixed with CdSe/CdS QD aqueous solution, the obviously enhanced QD fluorescent emission was detected. As seen from Fig. 6c and Fig. 6d, the Au/Ag NPs with thicker SiO_2 layer exhibited stronger enhanced MEF effects, especially for the bimetallic nanoparticles subject to silica coating for 24 h, the silica layer thickness was found to be ~30 nm from TEM inset, the fluorescent emission intensity of QD in the presence of Au/Ag nanoparticles was increased up to 200 a.u., which is much larger than that of pure QD (around ~60 a.u.), while the Au/Ag NPs grafted with thin silica layer (silica coating for 6h, thickness of ~ 4 nm) still quenched the QD fluorescence (data not shown). Although only 3 times fluorescent enhancement at 560 nm was obtained from the CdSe/CdS QD-Au@Ag@SiO_2 aqueous mixture (60:40 volume ratio) for the moment, we assume that the MEF factor will be amplified by optimizing morphology, spectral overlap, surface modification protocols and relative loading concentrations of QD and bimetallic nanocubes, these detailed work are currently in progress.

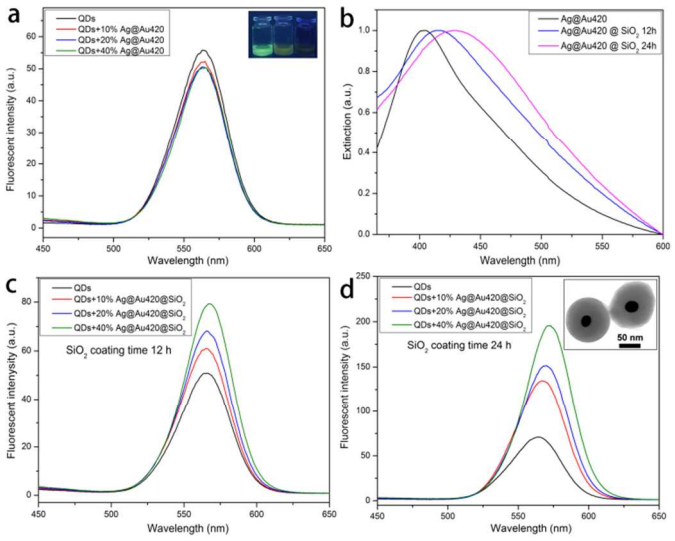

Fig. 6 Fluorescent emission spectra of water soluble QDs in the presence of different content of Au/Ag bi-metallic NPs, shown in upper-right inset was the solution containing QDs in n-hexane, water and in the presence of Au/Ag NPs in water (from left to right) under 365 nm light illumination, the UV-Vis spectra of silica modified Au/Ag NPs (b) and enhanced fluorescent emission from QD aqueous solution in the presence of silica modified Ag/Au NPs (c, d), the TEM morphology of Au/Ag nanoparticles after 24 h silica coating was shown in upper-right inset of (d), the excitation wavelength was 365 nm and all the emission spectra were recorded in water.

Conclusions

In this work, the monodispersed gold/silver bimetallic nanoparticles have been synthesized via a one-pot co-reduction of $HAuCl_4$ and $AgNO_3$ by DMF in the presence of PVP. The size and morphology of bimetallic Au/Ag NPs can be modulated by changing different experimental conditions (i.e. reaction time and relative concentration ratio of gold/silver ions precursors). In order to explore the plasmonic modulated fluorescence ability of the bimetallic nanoparticles, the highly luminescent CdSe/CdS quantum dots (QD) have been synthesized and admixed with as-synthesized gold/silver nanoparticles and silica modified Au/Ag NPs, respectively. The fluorescent experiments including steady fluorescent spectroscopy and transient fluorescent lifetime measurement confirmed that the strong quenching effects of unmodified Au/Ag NPs to QD fluorescence was attributed to the resonant energy transfer from QD to bimetallic plasmonic nanostructures, while the obviously enhanced fluorescence of QD by the silica modified Au/Ag NPs was due to the near-field optical enhancement of plasmonic nanostructures. The experimental results in the present work are obtained directly from liquid mixtures of quantum dots and plasmonic nanostructures, which would consolidate the understanding of plasmon mediated QD fluorescence in the colloid solution.

Acknowledgements

The authors gratefully thank the financial support from National Natural Science Foundation of China (Project No.

51373028, No. 51403029), "863"National Major Program of High Technology (2012AA03A212), South Wisdom Valley Innovative Research Team Program, Ningbo Major (key) Science and Technology Research Plan (2013B06011) and the Fundamental Research Funds for the Central Universities (ZYGX2013J121). The authors also appreciate Prof. Chunhui Wu from School of Life Science and Technology at UESTC and Dr. Yumin Huang from Sichuan University for their kind assistance in the fluorescent spectroscopy measurements.

Notes and references

[a] Research Branch of Advanced Functional Materials, High Temperature Resistant Polymer and Composites Key Laboratory of Sichuan Province, School of Microelectronics and Solid-State Electronics, University of Electronic Science and Technology of China, Chengdu, 610054, P. R. China. E-mail: jiakun@uestc.edu.cn (K. Jia), liuxb@uestc.edu.cn (X. B. Liu), Tel: +86-28-83207326, Fax: +86-28-83207326.

[b] School of Resources and Environment, University of Electronic Science and Technology of China, Chengdu, 610054, China.

[c] Kun Jia and Liting Yuan contribute equally to this work.

1. M. B. Cortie and A. M. McDonagh, *Chem. Rev.*, 2011, **111**, 3713-3735.
2. A. Klinkova, R. M. Choueiri and E. Kumacheva, *Chem. Soc. Rev.*, 2014, **43**, 3976-3991.
3. D. Lin, S. Feng, H. Huang, W. Chen, H. Shi, N. Liu, L. Chen, W. Chen, Y. Yu and R. Chen, *J. Biomed. Nanotech.*, 2014, **10**, 478-484.
4. E. Ringe, B. Sharma, A.-I. Henry, L. D. Marks and R. P. Van Duyne, *Phys. Chem. Chem. Phys.*, 2013, **15**, 4110-4129.
5. K. Jia, J. L. Bijeon, P. M. Adam and R. E. Ionescu, *Analyst*, 2013, **138**, 1015-1019.
6. T. Ming, H. Chen, R. Jiang, Q. Li and J. Wang, *J. Phys. Chem. Lett.*, 2011, **3**, 191-202.
7. K. Jia, J. L. Bijeon, P. M. Adam and R. E. Ionescu, *Plasmonics*, 2013, **8**, 143-151.
8. K. Jia, J. L. Bijeon, P. M. Adam and R. E. Ionescu, *Anal. Chem.*, 2012, **84**, 8020-8027.
9. L. Zhao, T. Ming, L. Shao, H. Chen and J. Wang, *J. Phys. Chem. C*, 2012, **116**, 8287-8296.
10. Y. Peng, B. Xiong, L. Peng, H. Li, Y. He and E. S. Yeung, *Anal. Chem.*, 2015, **87**, 200-215.
11. Z. Tang and A. Wei, *ACS Nano*, 2012, **6**, 998-1003.
12. O. S. Wolfbeis, *Chem. Soc. Rev.*, 2015, DOI: 10.1039/C4CS00392F.
13. Y.-Q. Li, L.-Y. Guan, H.-L. Zhang, J. Chen, S. Lin, Z.-Y. Ma and Y.-D. Zhao, *Anal. Chem.*, 2011, **83**, 4103-4109.
14. S. Dey, Y. Zhou, X. Tian, J. A. Jenkins, O. Chen, S. Zou and J. Zhao, *Nanoscale*, 2015, **7**, 6851-6858.
15. P. Wang, L. T. Yuan, X. Huang, W. J. Chen, K. Jia and X. B. Liu, *RSC Adv.*, 2014, **4**, 46541-46544.
16. D. Yang, Q. Chen and S. Xu, *J. Lumin.*, 2007, **126**, 853-858.
17. X. Wang, J. Zhuang, Q. Peng and Y. Li, *Nature*, 2005, **437**, 121-124.
18. Z. A. Peng and X. Peng, *J. Am. Chem. Soc.*, 2001, **123**, 1389-1395.
19. Z. A. Peng and X. Peng, *J. Am. Chem. Soc.*, 2002, **124**, 3343-3353.
20. M. Li, J. Ouyang, C. I. Ratcliffe, L. Pietri, X. Wu, D. M. Leek, I. Moudrakovski, Q. Lin, B. Yang and K. Yu, *ACS Nano*, 2009, **3**, 3832-3838.
21. Y.-H. Chan, J. Chen, S. E. Wark, S. L. Skiles, D. H. Son and J. D. Batteas, *ACS Nano*, 2009, **3**, 1735-1744.
22. A. Demortière, R. D. Schaller, T. Li, S. Chattopadhyay, G. Krylova, T. Shibata, P. C. dos Santos Claro, C. E. Rowland, J. T. Miller, R. Cook, B. Lee and E. V. Shevchenko, *J. Am. Chem. Soc.*, 2014, **136**, 2342-2350.
23. N. M. Kha, C.-H. Chen, W.-N. Su, J. Rick and B.-J. Hwang, *Phys. Chem. Chem. Phys.*, 2015, DOI: 10.1039/C4CP05217J.
24. K. Munechika, Y. Chen, A. F. Tillack, A. P. Kulkarni, I. J.-L. Plante, A. M. Munro and D. S. Ginger, *Nano. Lett.*, 2010, **10**, 2598-2603.
25. H. Naiki, S. Masuo, S. Machida and A. Itaya, *J. Phys. Chem. C*, 2011, **115**, 23299-23304.
26. E. Margapoti, D. Gentili, M. Amelia, A. Credi, V. Morandi and M. Cavallini, *Nanoscale*, 2014, **6**, 741-744.
27. B. Ji, E. Giovanelli, B. Habert, P. Spinicelli, M. Nasilowski, X. Xu, N. Lequeux, J.-P. Hugonin, F. Marquier, J.-J. Greffet and B. Dubertret, *Nat. Nano.*, 2015, **10**, 170-175.
28. N. S. Karan, A. M. Keller, S. Sampat, O. Roslyak, A. Arefin, C. J. Hanson, J. L. Casson, A. Desireddy, Y. Ghosh, A. Piryatinski, R. Iyer, H. Htoon, A. V. Malko and J. A. Hollingsworth, *Chem. Sci.*, 2015, **6**, 2224-2236.
29. S. Y. Lee, K. Nakaya, T. Hayashi and M. Hara, *Phys. Chem. Chem. Phys.*, 2009, **11**, 4403-4409.
30. M. Ramirez-Maureira, V. c. V. C, A. Riveros, P. J. G. Goulet and I. O. Osorio-Roman, *Mater. Chem. Phys.,* 2015*,* **151**, 351-356.
31. I. C. Serrano, C. Vazquez-Vazquez, A. M. Adams, G. Stoica, M. A. Correa-Duarte, E. Palomares and R. A. Alvarez-Puebla, *RSC Adv.*, 2013, **3**, 10691-10695.
32. O. Kulakovich, N. Strekal, A. Yaroshevich, S. Maskevich, S. Gaponenko, I. Nabiev, U. Woggon and M. Artemyev, *Nano. Lett.*, 2002, **2**, 1449-1452.
33. R. Li, S. Xu, C. Wang, H. Shao, Q. Xu and Y. Cui, *ChemPhysChem*, 2010, **11**, 2582-2588.
34. A. E. Ragab, A. S. Gadallah, T. Da Ros, M. B. Mohamed and I. M. Azzouz, *Opt. Commun.*, 2014, **314**, 86-89.
35. C. Rohner, I. Tavernaro, L. Chen, P. J. Klar and S. Schlecht, *Phys. Chem. Chem. Phys.*, 2015, **17**, 5932-5941.
36. H. F. Zarick, W. R. Erwin, J. Aufrecht, A. Coppola, B. R. Rogers, C. L. Pint and R. Bardhan, *J. Mater. Chem. A*, 2014, **2**, 7088-7098.
37. Y.-C. Tsao, S. Rej, C.-Y. Chiu and M. H. Huang, *J. Am. Chem. Soc.*, 2014, **136**, 396-404.
38. S. Xing, L. H. Tan, T. Chen, Y. Yang and H. Chen, *Chem. Commun.*, 2009, 1653-1654.
39. C. Li, L. Sun, Y. Sun and T. Teranishi, *Chem. Mater.*, 2013, **25**, 2580-2590.
40. L. Polavarapu and L. M. Liz-Marzan, *Nanoscale*, 2013, **5**, 4355-4361.
41. Y. Yang, W. Wang, X. Li, W. Chen, N. Fan, C. Zou, X. Chen, X. Xu, L. Zhang and S. Huang, *Chem. Mater.*, 2013, **25**, 34-41.
42. K. Jia, M. Y. Khaywah, Y. Li, J. L. Bijeon, P. M. Adam, R. Déturche, B. Guelorget, M. François, G. Louarn and R. E. Ionescu, *ACS Appl. Mater. Interfaces*, 2014, **6**, 219-227.
43. K. Jia, P. Wang, L. Yuan, X. Zhou, W. Chen and X. Liu, *J. Mater. Chem. C*, 2015, **3**, 3522-3529.
44. I. Pastoriza-Santos and L. M. Liz-Marzán, *Langmuir*, 2002, **18**, 2888-2894.

45. Q. Zhang, W. Li, L.-P. Wen, J. Chen and Y. Xia, *Chem. Eur. J.*, 2010, **16**, 10234-10239.
46. S. Peng and Y. Sun, *Chem. Mater.*, 2010, **22**, 6272-6279.
47. L. Carbone, A. Jakab, Y. Khalavka and C. Sönnichsen, *Nano. Lett.*, 2009, **9**, 3710-3714.
48. H. Liu, Y. Feng, D. Chen, C. Li, P. Cui and J. Yang, *J. Mater. Chem. A*, 2015, **3**, 3182-3223.
49. M. Focsan, A. M. Gabudean, A. Vulpoi and S. Astilean, *J. Phys. Chem. C*, 2014, **118**, 25190-25199.
50. G. Sagarzazu, K. Inoue, M. Saruyama, M. Sakamoto, T. Teranishi, S. Masuo and N. Tamai, *Phys. Chem. Chem. Phys.*, 2013, **15**, 2141-2152.
51. Y. Tang, Q. Yang, T. Wu, L. Liu, Y. Ding and B. Yu, *Langmuir*, 2014, **30**, 6324-6330.
52. V. Reboud, G. Leveque, M. Striccoli, T. Placido, A. Panniello, M. L. Curri, J. A. Alducin, T. Kehoe, N. Kehagias, D. Mecerreyes, S. B. Newcomb, D. Iacopino, G. Redmond and C. M. S. Torres, *Nanoscale*, 2013, **5**, 239-245.

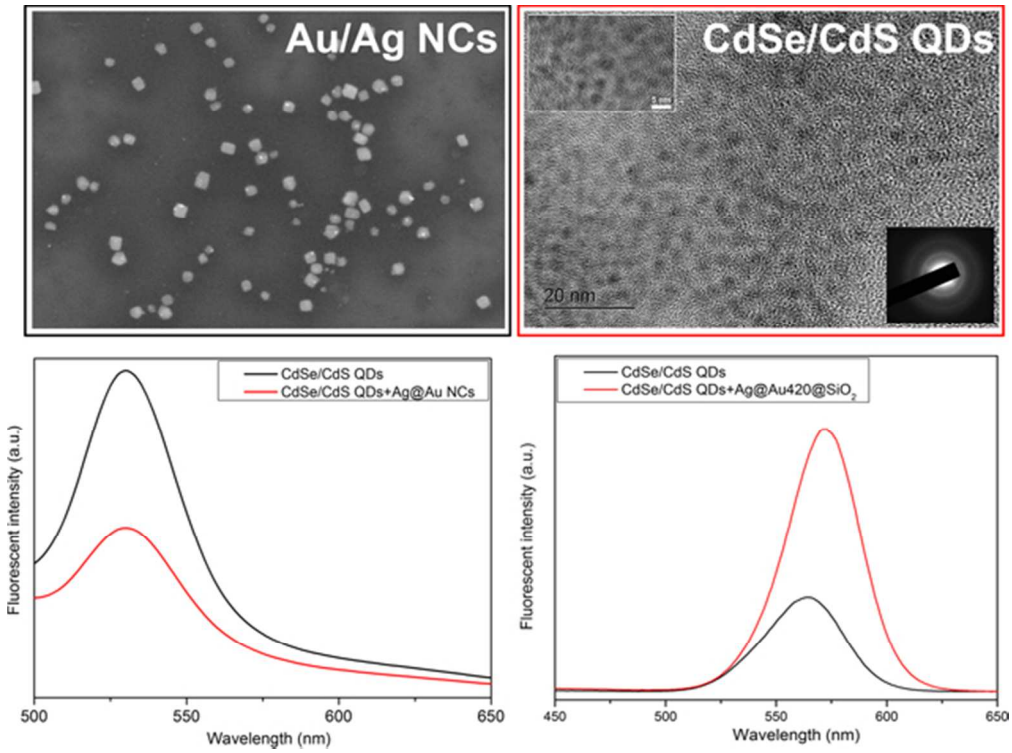

Fluorescent emission of CdSeCdS nanocrystals in colloid solution can be effectively modulated by AuAg bimetallic nanoparticles.
53x39mm (300 x 300 DPI)